# Multifocal point beam forming by a single ultrasonic transducer with 3D printed holograms

Jun Zhang,[1,a),b)] Yang Yang,[2,a)] Benpeng Zhu,[3,4] Xiangjia Li,[2] Jie Jin,[2] Zeyu Chen,[2] Yong Chen,[2] and Qifa Zhou[3,5,c)]
[1]*School of Power and Mechanical Engineering, Wuhan University, Hubei, Wuhan 430072, China*
[2]*Epstein Department of Industrial and Systems Engineering, University of Southern California, Los Angeles, California 90089, USA*
[3]*USC Roski Institute, Keck School of Medicine, University of Southern California, Los Angeles, California 90033, USA*
[4]*School of Optical and Electronic Information, Huazhong University of Science and Technology, Wuhan 430074, China*
[5]*Department of Biomedical Engineering, University of Southern California, Los Angeles, California 90089, USA*

(Received 16 September 2018; accepted 26 November 2018; published online 11 December 2018)

This paper reported a method for designing monolithic acoustic holograms with consideration of both amplitude and phase modulation, which can be used for multifocal point beam forming by a single element ultrasonic transducer in the frequency of megahertz range. Mask-image-projection-based stereolithography 3D printing technology was induced to manufacture the complex hologram with a pixel resolution of 25 $\mu$m. A nine foci pattern and a letter U pattern acoustic field shown by a 2 MHz transducer and holograms were designed to validate the proposed designing method. Both the hydrophone testing and the simulation results indicated that the holograms designed by our method could form beam patterns accurately in the expected position. *Published by AIP Publishing.*
https://doi.org/10.1063/1.5058079

Acoustic holograms are efficient tools for wave manipulation and have been already used in many fields in recent years, such as acoustic assembly, trapping and levitation, neural stimulation, as well as ultrasound imaging.[1–5] An acoustic metasurface is designed to be an array of phase and/or amplitude profiles that are capable of generating complex wavefront by interference of each element source. A phased array ultrasonic system is easy to produce steerable and focused beams by only modulating the delay law of each element.[6] However, in order to form an arbitrary ultrasonic beam, thousands of elements with a sub-wavelength size are needed for an independent transducer, which will lead to a high cost ultrasonic system and transducer making. Monolithic acoustic holograms can also generate complex beam patterns emitted by a single element transducer with a reasonable designed phase and amplitude profile. Then, the thickness of each acoustic pixel in the hologram will affect both the phase and the amplitude used for interference field reconstruction. So, the computer generated hologram (CGH) algorithm for acoustic profile design is extremely important and more difficult than delay law design of phased array transducers. The manufacture of a hologram with a complex surface and a high resolution is equally important.

The CGH algorithms were first induced in the optical field, such as the iterative angular spectrum approach (IASA), the Fourier-based algorithm, the finite difference discretization, and the weighted Gerchberg-Saxton (GSW) algorithm.[7–9] Then, the algorithms for designing acoustic holograms were proposed by adapting ideas from optical computer generated holography. Hertzberg *et al.* compared the performance of four CGH algorithms for multifocal acoustics frameworks to neural pattern stimulation applications and found the GSW overall superior efficiency and uniformity in the focal spots.[10] An angular spectrum-GSW method was also validated for efficient generation of complex acoustic images which gave a powerful solution for ultrasonic retina stimulation.[11] Xie *et al.* modified the GSW algorithm to generate the optimal phased distribution in the low frequency sound range (~4 kHz) with 180°of phase delay.[12] Wu *et al.* proposed a 2D Fourier transform (FT) algorithm for acoustic pattern generation and integrated with a circularly shaped 2D CMUT array which could be placed in front of the eye to project acoustic images onto the retina dynamically.[13] However, these algorithms are phase-only modulation limited in ultrasonic phased arrays. Melde *et al.* used the transmission coefficient between the transducer and the medium to modify the IASA and designed monolithic acoustic holograms which can reconstruct diffraction-limited fields and thus arbitrary ultrasound patterns.[14] Zhu showed a decoupled amplitude phase modulation instead of the phase-controlled approach to design holey structured lossy metamaterials.[15]

In this work, we introduced a modified GSW method for monolithic acoustic hologram design with consideration of both amplitude and phase modulation. The 3D printing technology was induced to manufacture the hologram with a complex surface in the frequency of megahertz range. Additive manufacturing (3D printing) is one of the effective ways to fabricate customized parts with complicated architecture and has a wide application in industry, academia, and daily usages. A hydrophone system was used to measure the

[a)]J. Zhang and Y. Yang contributed equally to this work.
[b)]Electronic mail: zhangjun2010@whu.edu.cn
[c)]Electronic mail: qifazhou@usc.edu

acoustic pattern in water. The results show that our approach could finely manipulate the 3D ultrasonic fields with a simple design, low-cost fabrication, monolithic hologram, and single element transducer.

The hologram which is mounted on the surface of the ultrasonic transducer is used to modulate the amplitude and the phase of the emitted acoustic field. Then, the designed pressure pattern is generated by the interference of each pixel on the digital hologram. The size of the pixel is an important parameter which determines the scalar–space bandwidth product (SW) for a fix single element transducer. Holograms with a small pixel size lead to higher SW and make the field reconstructions with a larger spatial extent and finer detail.[14] The pixel size should be smaller than the half of the wavelength due to the diffraction limitation. For example, for a 5 MHz transducer with a diameter of 30 mm immersed in water, the wavelength is 300 $\mu$m and the SW is about 7850, much larger than a phased array transducer.

The acoustic pattern can be described as a series of focal points, and so, we note $P(r_m)$ as the acoustic field of the focal points (targets) in the propagation medium on the focal plane. The transducer surface can be described as many vibrating points with the amplitude of $A_n$ and the phase of $\varphi_n$. The acoustic field of each focal point can be calculated by the Rayleigh-Sommerfeld integral

$$P(r_m) = \sum A_n \exp(j\phi_n - jkD_{mn})/D_{mn}, \tag{1}$$

where $D_{mn}$ is the distance between the point source n and the target m. k is the wavenumber of the ultrasound in the medium.

Two parameters are used to quantify the performance of the focal patterns. The first is Normalized efficiency which is an estimate of the power delivered to the mth target, computed over L pixels that cover the focal point

$$e_m = \frac{1}{P_m}\sum_m \left(S\sum_{i=1}^{L} P_{m,i}\right). \tag{2}$$

The second parameter is the Uniformity of power delivery to the targets

$$u_m = \frac{2}{\max(S\sum_{i=1}^{L} P_{m,i})/\min(S\sum_{i=1}^{L} P_{m,i}) + 1}. \tag{3}$$

The GSW method is an extension of GS which maximizes a similar weighted sum of magnitudes delivered to the focal points and results in a weighted iteration formula

$$\phi_n^i = \arg\left[\sum_m w_m^i \exp(jkD_{mn})P_m^{i-1}/|P_m^{i-1}|\right]. \tag{4}$$

As for the holograms of single element ultrasonic transducers, the phase modulation is controlled by the thickness profile hologram plate and the difference of the wavenumber in propagation medium and holograms

$$\phi_n = (k - k_h)T_n. \tag{5}$$

Furthermore, the attenuation of different propagation distances and the transmission in the multilayered system composed of transducers, holograms, and medium must be considered. This means that the amplitude modulation is needed during the iteration. The transmission coefficient $\alpha_n^{i-1}$ was described in Ref. 13. A modified GSW method with a hologram thickness and attenuation is proposed for single element transducer hologram designing.

$$\begin{aligned} T_n^i &= \arg\left[\sum_m w_m^i \exp(jkD_{mn})P_m^{i-1}/|P_m^{i-1}|\right]/(k - k_h) \\ P_m^{i-1} &= \sum \alpha^{i-1} \exp\left[j(k - k_h)T_n^{i-1} - jkD_{mn}\right]/D_{mn}. \end{aligned} \tag{6}$$

As the iteration attempts to maximize the efficiency and uniformity of the patterns, we can define a relative uniformity parameter and the convergence condition

$$\begin{aligned} \delta_u^i &= \left[\frac{u_m^i - u_m^{i-1}}{u_m^{i-1}}\right], \quad \delta_e^i = \left[\frac{e_m^i - e_m^{i-1}}{e_m^{i-1}}\right] \\ \delta^i &= \max(\delta_u^i, \delta_e^i). \end{aligned} \tag{7}$$

There are many numerical simulation tools that can be used to verify the designed holograms. Here, we chose a well-established technique, Angular Spectrum approach (ASA) with simplicity and high efficiency to simulate the acoustic pattern generated by the designed hologram.

The self-made ultrasonic transducer is composed of a PZT element with a diameter of 30 mm and a frequency of 2 MHz and a backing layer made of a very lossy conductive epoxy (E-Solder 3022, Von Roll Isola Inc., New Haven, CT) with an acoustic impedance of 6 MRayl, matching layer made by mixing of $Al_2O_3$ and epoxy with an acoustic impedance of 2.7 MRayl. The material of the designed hologram is a kind of resin with Young's modulus of 2500 MPa and Poisson's ratio of 0.41. The matching layer, acoustic hologram, and water comprises a multi-layered propagation medium with different acoustic impedance and attenuation (Figs. 1 and 2).

The designed holograms for the multi-foci and letter pattern are shown in Figs. 3 and 4, with a spacing grid of 200 $\mu$m. The diameter of the hologram area is 30 mm, the same as the transducer element. The nine points in the focal plane were set with a spacing of 8 mm, covering an area of $16 \times 16\,\text{mm}^2$. The focal plane was set 60 mm away from the front of the surface. From the simulated acoustic field in Figs. 4(b) and 4(c), we can see that the hologram has divided the beam into nine beams, and each beam has foci on the 60 mm plane. Letter U was chosen to verify the designing method. Letter U was set by 64 evenly distributed points with a height of 16 mm and a width of 20 mm. From the simulated field in Fig. 5(c), we can found that U was clearly

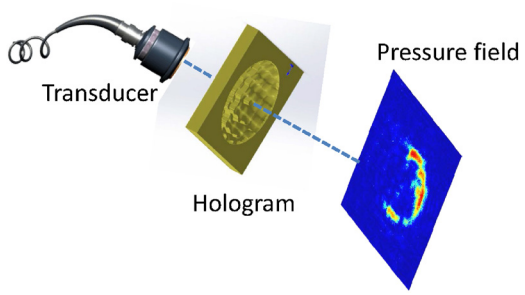


FIG. 1. Illustration of the use of holograms to generate acoustic patterns.

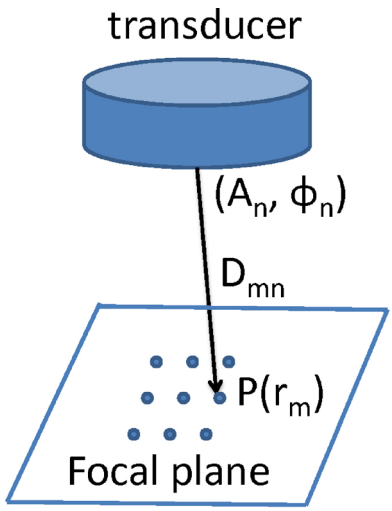


FIG. 2. Illustration of point sources on the transducer's surface and targets on the focal plane.

formed. The chosen letter is asymmetric and continuous which makes it a good test of the proposed designing method.

The hologram was manufactured by the stereolithography apparatus (SLA) 3D printing method with the material of future 8000 resin. The SLA is a widely used method for fabricating complex geometry of plastics and ceramics with the advantage of very high resolution. The SLA with a resolution of 25 $\mu$m could support the manufacture of holograms for a single transducer limited to a frequency of 30 MHz. For a 2 MHz transducer emitted in water, the wavelength is 750 $\mu$m, and so, it is enough to manufacture the hologram which is designed with a spacing of 200 $\mu$m.

A mask-image-projection-based stereolithography (MIP-SL) process is used due to its high-quality surface finish, dimensional accuracy, high fabrication speed, and low machine cost. Different from a laser-based stereolithography (SLA), a digital micromirror device (DMD) is used in the MIP-SL process to dynamically define mask images that are projected on a photocurable resin surface (Fig. 3). The acoustic hologram model was first created using matlab and Solidworks [Fig. 3(a)] and then sliced by in-house developed "DMD-based SL" software [Fig. 3(b)] to get different patterns [Fig. 3(c)]. Those patterns were then projected to build different layers. For example, the first layer was built by projecting the first pattern until the 46th layer was obtained [Fig. 3(c)]. For the fabrication process, different patterns would be projected on the surface of photocurable resin. The resin would become solidified due to its photocurable property. After the first layer was cured on the base, the base would move up and then move down for the second layer to be projected and so on. The curing time of each layer was 2 s, and the movement of the base took about 5 s. During the movement, the layer thickness is controlled to be less than the cure depth to make sure that the following layer is stick onto the previous layers. In our study, the movement in the z-direction was controlled to be 25–100 $\mu$m and the cure depth was about 300 $\mu$m for 2 s. The output light intensity is 3.16 mW/cm$^2$.

A hydrophone system was used to measure the acoustic field generated by the holograms. The hologram was fixed on the surface of the transducer. Both of them were then immersed in water approximately 60 mm away from the testing plane. The hydrophone was aligned to the center of the transducer by the motor controller (ESP301, Newport) and scanned horizontally with a step of 200 $\mu$m over an area of 40 mm $\times$ 40 mm. The pulser/receiver (Panametrics 5900PR, Olympus, Waltham, MA) with a bandwidth from 1 MHz to 100 MHz was used to transmit and receive ultrasound signals. The sampling frequency of the high-speed acquisition card used to acquire the signal was set to 1 GHz.

The measured acoustic field is shown in Figs. 4(d) and 5(d). In both cases, the designed pattern U and nine points have been clearly realized and the two show excellent agreement with the simulated field in the overall shape of the pattern. In order to check the uniformity of the generated pattern, the focal tightness of nine points in horizontal and vertical axes is plotted in Figs. 4(e) and 4(f). It is obvious that the intensities of nine points were equally distributed.

It is proved that the 3D printed hologram is an efficient tool for acoustic field manipulation. The surface profile is

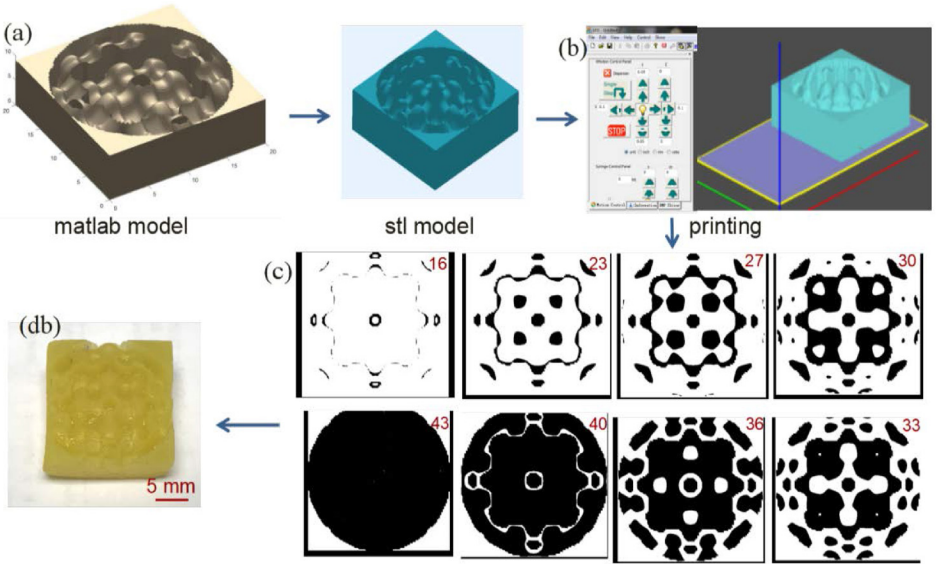


FIG. 3. 3D printing process of the acoustic hologram: (a) Matlab model and STL model; (b) printing procedure designing; (c) layer during printing; (d) 3D printed hologram.

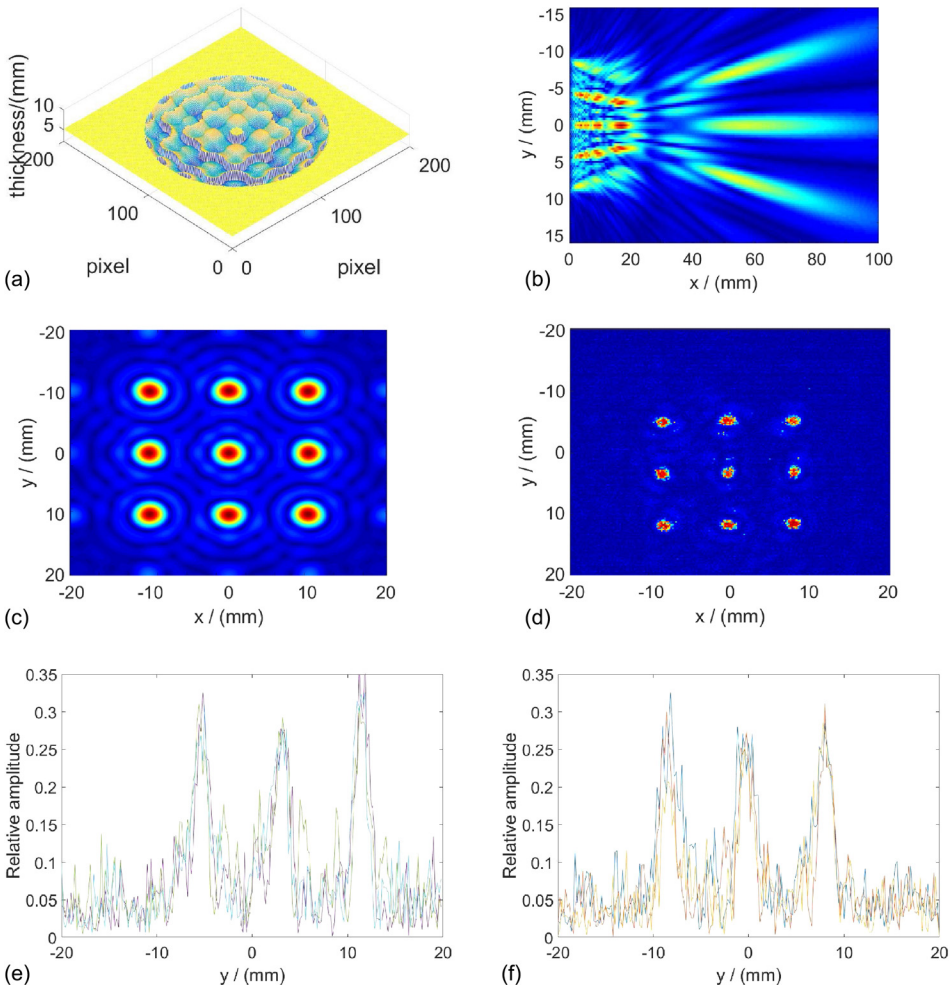


FIG. 4. Multifoci acoustic field generation: (a) hologram profile plotted by matlab; (b) simulated acoustic field in the x-z plane; (c) simulated acoustic field in the x-y plane; (d) measured acoustic field in the x-y plane; (e) measured acoustic field in the x-y plane; (f) measured acoustic field in the x-y plane.

dominated by the acoustic properties of the hologram materials. For example, there are many kinds of materials that can be manufactured by SLA 3D printing to formulate a plastic hologram, such as future 8000, make juice and SI500. The thickness range of the hologram pixel would vary in a wide range. For example, if the density and acoustic velocity of the material are close to the water medium, then a large thickness range is needed to provide the phased delay of each pixel on the hologram. Then, it is hard to accurately control the size of the peak area of the surface profile during the manufacturing process. If the density and acoustic velocity of the holographic material are much different from those

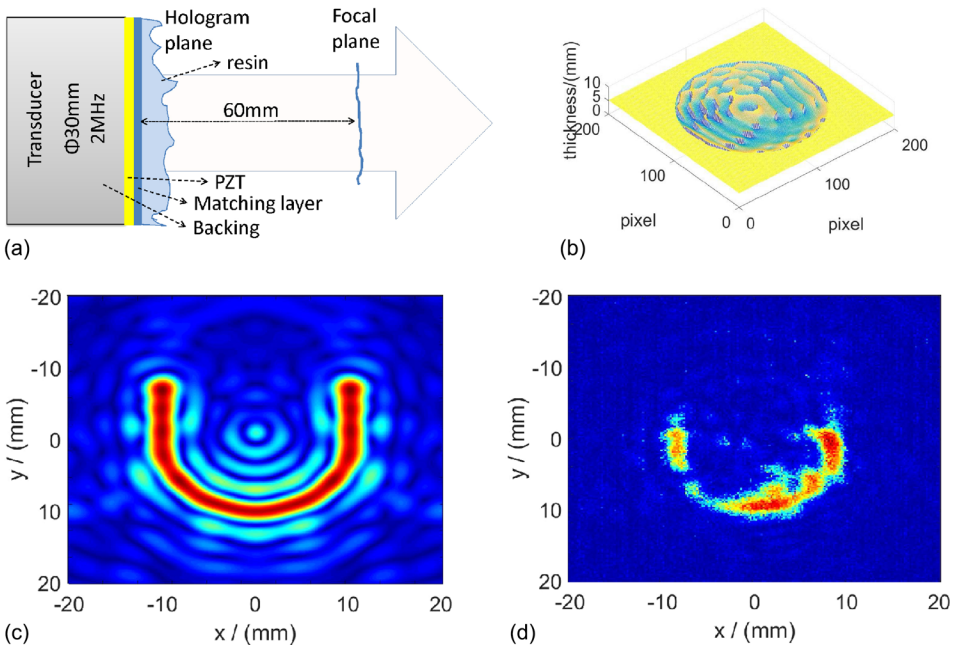


FIG. 5. Letter U pattern acoustic field generation: (a) configuration; (b) hologram profile; (c) simulated acoustic field in the x-y plane; (d) measured acoustic field in the x-y plane.

of the medium, the thickness range maybe on the micrometer scale which will exceed the limitation of SLA equipment. In this paper, the future 8000 material with a density of 1300 kg/m$^3$ and a velocity of 2114 m/s, showed excellent adaptability for holograms.

In this paper, both the nine-point hologram and the letter U hologram were designed with a spacing of 200 $\mu$m and a pixel number of 200 $\times$ 200. The size of the 6 dB focal point is about 1.2–1.6 mm. However, as the proposed method for computation is straightforward, increasing the hologram apertures and fining the pixel sizes will not add any other complexity. The smaller pixel size will store more phase information and make it possible to maintain high reconstruction fidelity. The 3D sculpting of the acoustic field will be realized when multiple image planes with distinct intensity distributions were encoded in a single hologram.

In summary, this paper has demonstrated that complex acoustic patterned distributions can be generated using tailored holograms with specific surface profiles and a single element ultrasonic transducer. A modified GSW method for the design of these profiles for the generation of arbitrary acoustic field patterns has been introduced. It has also been shown that the designed profiles can be easily and accurately manufactured by the stereolithography apparatus (SLA) based 3D printing method, which is a widely used technique for plastic material making. In a word, many applications based on acoustic manipulation would benefit from the arbitrary wavefront generation by a monolithic acoustic hologram.

This work was supported by the National Key R&D Program of China (Grant No. 2018YFB1106100). This work was also supported by NIH Grant Nos. R01EY026091 and P41-EB2002182.

[1]H. Ge, M. Yang, C. Ma, M.-H. Lu, Y.-F. Chen, N. Fang, and P. Sheng, Nat. Sci. Rev. **5**(2), 159–182 (2018).
[2]K. Melde, E. Choi, Z. Wu, S. Palagi, T. Qiu, and P. Fischer, Adv. Mater. **30**(3), 1704507 (2018).
[3]A. Marzo, S. A. Seah, B. W. Drinkwater, D. R. Sahoo, B. Long, and S. Subramanian, Nat. Commun. **6**, 8661 (2015).
[4]B. W. Drinkwater and P. D. Wilcox, NDT & E Int. **39**(7), 525–541 (2006).
[5]Y. Hertzberg and G. Navon, Med. Phys. **38**(12), 6407–6415 (2011).
[6]L. R. Gavrilov, J. W. Hand, and I. G. Yushina, Acoust. Phys. **46**(5), 551–558 (2000).
[7]G. P. Nordin and S. D. Mellin, Opt. Express **8**(13), 705 (2001).
[8]R. D. Leonardo, F. Ianni, and G. Ruocco, Opt. Express **15**(4), 1913–1922 (2007).
[9]A. Lotfi, T. E. Simos, G. Psihoyios, and C. Tsitouras, AIP Conf. Proc. **936**, 351–355 (2007).
[10]Y. Hertzberg, O. Naor, A. Volovick, and S. Shoham, J. Neural Eng. **7**(5), 056002 (2010).
[11]O. Naor, Y. Hertzberg, E. Zemel, E. Kimmel, and S. Shoham, J. Neural Eng. **9**(2), 026006 (2012).
[12]Y. Xie, C. Shen, W. Wang, J. Li, D. Suo, B. I. Popa, Y. Jing, and S. A. Cummer, Sci. Rep. **6**, 35437 (2016).
[13]X. Wu, M. Kumar, and ß. Oralkan, in *Ultrasonics Symposium* (2014), Vol. 2623, p. 2626.
[14]K. Melde, A. G. Mark, T. Qiu, and P. Fischer, Nature **537**(7621), 518–522 (2016).
[15]Y. Zhu, J. Hu, X. Fan, J. Yang, B. Liang, X. Zhu, and J. Cheng, Nat. Commun. **9**(1), 1632 (2018).